

Automated and generalized integral-field spectroscopy data reduction using p3D

Christer Sandin, Peter Weilbacher, Fachreddin Tabataba-Vakili, Sebastian Kamann, Ole Streicher
Leibniz Institute for Astrophysics Potsdam (AIP), An der Sternwarte 16, 14482 Potsdam, Germany

ABSTRACT

Integral-field spectrograph (IFS) instruments are well suited to observe extended and faint objects, such as planetary nebulae and galaxies. A result of such observations are large quantities of raw data, which mostly require an expert to derive accurate scientific spectra. Most instruments handle up to several thousand spectra simultaneously, using a unique file format, together with numerous instrument-specific issues, which only an experienced expert can resolve. p3D is an open source processing tool that is designed to handle raw data of any fiber-fed IFS, reducing IFS data quickly, easily, and accurately. Separate tools are available that handle many tasks including cosmic-ray hit rejection in single spectrum images, the combination of images, tracing of spectra on the detector, determination of spatial profiles of any shape, handling of images for flat fielding, different versions of spectrum extraction, combination of multi-detector data, and correction for atmospheric differential refraction. The same approach and code is used with all instruments. No license is required when using p3D, even though it is based on the proprietary software IDL; this is made possible through precompiled binary files that are distributed together with the source code. p3D has been much improved with numerous releases since the first version early in 2010. Here we present the latest capabilities of a nearly complete program.

Keywords: methods: data analysis, methods: observational, techniques: spectroscopic

1. INTRODUCTION

p3D is an open-source tool for reduction of integral-field spectroscopy (IFS) data that was first released in February 2010.¹ This new code was completely restructured and rewritten, compared to earlier proprietary versions.² The first release of p3D supports both the LArr and the PPAK integral-field units (IFUs) of the PMAS instrument on the 3.5m telescope at Calar Alto, as well as the Spiral IFU at the AAO, and the Virus-P IFU at the McDonald 2.7 telescope. Five reduction tools are included to create: a master-bias image, a trace-mask image and a line-profiles image for optimal extraction using novel approaches, a dispersion-mask image for wavelength calibration, an image for flat-fielding of extracted data, and an extracted science-object image. Final output files can be studied in the separate graphical-user-interface (GUI) based spectrum viewer. Other GUIs are used to inspect the spectrum tracing and the spectrum extraction processes. p3D is software that is written in the interactive data language (IDL), which is proprietary software. Through the IDL virtual machine it is nevertheless possible to use p3D with full functionality without an IDL license.

There have been some limitations of the first version of p3D. It can only be accessed through a GUI; it would be helpful for repeated reductions if it could also be used from scripts. Spectra of non-working, low-transmission, and unused fibers are not treated differently than other spectra. Cosmic rays can only be removed through combination of three or more images. Effects of instrument flexure, which shift science-object data relative to calibration data, are neglected. Several tools are extremely slow. Since the original release p3D was improved during several releases to account for these issues. Support for additional instruments were added to broaden its applicability, and new tools were added to simplify reduction work and increase the quality of the reduced outcome further. Here we describe new major improvements and the large number of new tools that were added since the first release.

This paper is structured as follows. In Sect. 2 we describe general improvements to p3D, including support for additional instruments. In Sect. 3 we describe additions to already existing data-reduction tools, and in Sect. 4 we introduce new tools that were added since the p3D paper in 2010. Finally, in Sect. 5 we present conclusions and a brief outlook on the future.

Further author information: Send correspondence to C.S., E-mail: csandin@aip.de, Telephone: +49 (0)331 7499 675

2. GENERAL IMPROVEMENTS

All parts of p3d were written to minimize redundancy. This means both that the same routines are used to reduce data of all instruments, and that all improvements and modifications apply to all instruments on all supported platforms, which include Linux, Solaris, Mac OSX, and Windows. Moreover, each reduction tool is thoroughly documented in the file header, where a more nicely formatted version is available on the p3d web site*. General hints and tips regarding different instruments and reduction features, as well as recommended setups, are available on the p3d documentation wiki†.

In the following sections we discuss general improvements to p3d. At first we list the added instruments and their supported modes in Sect. 2.1, and make some notes on smaller general code improvements in Sect. 2.2. The improved user interface is discussed in Sect. 2.3, and the new C routines in Sect. 2.4.

2.1 New support for additional instruments

Internally, the only difference to p3d when it handles different instruments is how it reads raw data files. The data-reduction procedure nevertheless varies with the instrument due to instrument flexure, the configuration, and the IFU status in terms of, e.g., fully working spectra. In addition to the four IFUs that were supported previously, the following fiber-fed IFSs and IFUs are now also supported, or are considered for support in the near future:

ESO-VLT/UT3/VIMOS The “Visible MultiObject Spectrograph”

Both magnification scales of all four IFU modes, excluding the low-resolution modes, are supported: the medium-resolution grism (MR) as well as the three high-resolution grisms HR blue, HR orange, and HR red. Data from before and after the instrument refurbish in 2010 use different instrument-parameter files. The 1600 spectra are split onto four separate detectors, where the corresponding data files are reduced separately, before they are combined, cf. Sect. 4.3. The relatively large number of non-functional and low-transmission spectra are included in all output products, but are handled separately, and never compromise the quality of the reduced data.

ESO-VLT/UT2/FLAMES/Giraffe/ARGUS and IFU The “Fibre Large Array Multi Element Spectrograph”

Both plates with fifteen 20 square-element IFUs are supported, as well as the two magnification scales of the larger IFU ARGUS. Any of the 22 high-resolution setups and the eight low-resolution setups can be used; the wavelength range of each setup is identified automatically.

BTA 6m/MPFS The “Multi Pupil Fibre Spectrograph”

Data sampled using the newer 3k×2k CCD are supported. To add support for the older smaller CCD we would need data using it.

ERA2 This is a spectrograph at the AIP that is intended to be used in non-astronomy applications, mainly in life sciences.

Gemini North/GMOS-N and Gemini South/GMOS-S The two “Gemini Multi-Object Spectrographs”

All twelve grating setups of the integral field mode are supported in the one-slit setups, which use 500 science spectra and 250 sky spectra. Note, that when p3d combines images of the three detectors, empty space is left between the images, which correspond to the separation between the detectors.

WHT/WYFFOS/Integral All four IFUs – SB1, SB2, SB3, and equalized – are supported when using the older single CCD setup. Support is planned for the newer two-CCD setup in the near future.

Magellan/IMACS Due to a unique configuration using eight detectors that is tricky to handle, the IFS mode is not yet supported; although, future support is planned. As with all other instrument configurations the goal is to combine raw data of all eight detectors into one image. The combined images would then be used with p3d.

Virus-W This IFS is not yet supported. The instrument is based on the VIRUS spectrograph and is very similar to the VIRUS-P IFU, which is why it should be straightforward to add support for it.

*<http://p3d.sourceforge.net/index.php?page=doc>

†http://sourceforge.net/apps/mediawiki/p3d/index.php?title=Main_Page

Despite a significant increase in the number of supported and fiber-fed instruments, the full list of supported instruments is incomplete. Additional instruments can always be added, if raw data is provided. Moreover, except for the PMAS/LArr and the ERA2 IFUs, which both have a wide spectrum separation, it is strongly recommended to use a spectrum extraction method that corrects for overlapping spectra on the detector, or so-called cross-talk. However, this is only one of several corrections that might be necessary to reduce spectra accurately.

2.2 Notes on a few smaller general code improvements

Here are a few brief notes on some general improvements to `p3d`. It is since release 2.1.2 possible to use prescan and overscan regions instead of a master-bias image with all instruments that provide such regions in raw data. Furthermore, dispersion-mask images can be created with an already existing mask as template (2.0), and vignetted regions are ignored when fitting polynomials to create a dispersion-mask image (2.1.1). A one-dimensional drizzling algorithm³ is now used by default in the wavelength calibration. Finally, most tools now create postscript output files that can be used to inspect the quality of the reductions; these files allow a more automatic reduction procedure than a GUI.

2.3 Introducing a more versatile user interface

In the original release of `p3d` from 2010 all reduction tasks were called from a main graphical user interface (GUI) panel. Such an approach binds data-reduction tasks together, which are performed one by one, starting at the top of the GUI. The GUI also makes it easy to inspect results visually, through a click on the image-viewer button or the spectrum-viewer button. However, repeated reductions with the `p3d` GUI are tedious. Each file must be selected anew, including the user-parameter file. As `p3d` was constructed, it was also not possible to use the tool as a pipeline, without interaction.

`p3d` has been extended, and the various tools are now also accessible from the IDL command line, or from the shell. In the latter case there is no need to use an IDL license (when the provided pre-compiled binary files are used). In this case all options are set either using (available) keywords when calling the tool, or with “user parameters” in the user-parameter file. Repeated reductions are straightforward through the repeated execution of either a prepared shell script or a prepared IDL script. Most of the new tools that are described in Sect. 4 are unavailable in the GUI.

An example of both a shell script and an IDL script that are used with `p3d` are presented in The Messenger.⁴ Here are two examples that show how the spectrum viewer can be started. The example uses VIMOS data, and the session is started from the directory of the reduced data. Note that if the spatial map is to be shown properly, it is necessary to specify the IFU angle header keyword (`kwangle`) for instruments that allow non-zero angles, such as VIMOS (prior to release 2.2). The following commands could be used to start the spectrum viewer from the IDL command line:

```
IDL> d=readfits('504967_hr-blue_VIMOS.2010-11-03_crcl_oextr1_cal_vmcb.fits.gz',h)
IDL> dd=readfits('504967_hr-blue_VIMOS.2010-11-03_crcl_oextr1_cal_vmcb_err.fits.gz')
IDL> p3d_rss,d,dimage=dd,hdr=h,parfile='nvimos_hr.prm',[kwangle='HIERARCH ESO ADA POSANG']
```

The following commands could be used to start the spectrum viewer from the shell. In this case whitespace in the IFU angle header keyword must be replaced with a dash, due to the method that IDL uses to parse command-line options:

```
bash$ d=504967_hr-blue_VIMOS.2010-11-03_crcl_oextr1_cal_vmcb.fits.gz
bash$ dd=504967_hr-blue_VIMOS.2010-11-03_crcl_oextr1_cal_vmcb_err.fits.gz
bash$ kwangle=HIERARCH-ESO-ADA-POSANG
bash$ ${p3d_path}/vm/p3d_rss_vm.sh $d parfile=nvimos_hr.prm dimage=$dd [kwangle=$kwangle]
```

2.4 The addition of compiled C routines for increased speed of execution

`p3d` is coded in the interpreted interactive data language (IDL). Slow constructs such as loops can often be avoided through the use of intrinsic precompiled routines. This is not always the case; besides, IDL does not make use of multi-threaded CPUs, except in some simple routines. Some parts of `p3d` are computationally highly demanding, and require very long execution times when using the IDL routines. To decrease the reduction time, three routines have been ported to compiled C, where they are also parallelized using OpenMP, which by default makes use of all available CPU threads on the computer; fewer threads can be used, if required. The compilation of the C routines is automatic and the process is fully transparent to the user. Additionally, all files are compiled anew if any of the C routines is modified, for example after an update.

One of the three ported routines calculates cross-dispersion line profiles for optimal extraction. The fitting procedure involves up to several thousand free parameters, which are repeated across several wavelength bins. As an example, using

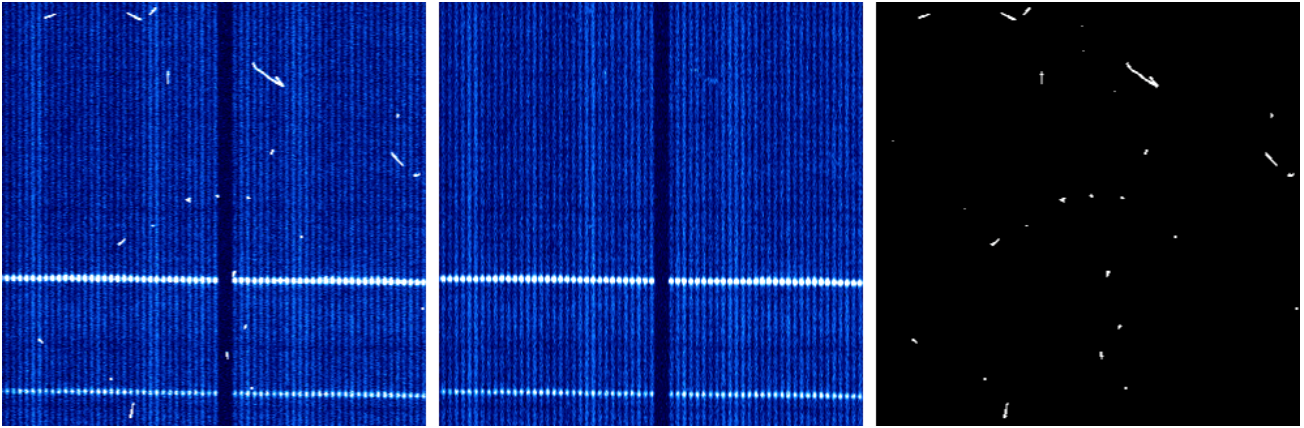


Figure 1. An example of a section of a VIMOS raw-data image that is cleaned of cosmic rays in `P3D` using the `pyCosmic` algorithm. From the left-hand side the three panels show: the raw image, the cosmic-ray cleaned image, and the cosmic-ray mask. Each vertical line is a spectrum. From the bottom the two horizontal “dotted” lines represent object emission in $O[III]\lambda\lambda 4959, 5007$.

eight threads (one thread) on an Intel Core i7 2.93GHz CPU it takes about 670, 730, 950, and 500 s (4100, 4500, 5800, and 3000 s) to calculate all properties of some 400 spectra for 206 wavelength bins for each of the four detectors. The corresponding times using the IDL routine are 6500, 7100, 9300, and 4700 s, which is 9.4–9.8 times slower than with the parallelized C routine. Note, however, that with a single thread the speedup is about 37%; hence, porting to C is in this case was mostly motivated by the speedup that is achieved through parallelization.

The other two ported routines are: the calculation of a median image for scattered-light correction, cf. Sect. 3.4; and optimal spectrum extraction, with the method that uses the so-called multi-profile deconvolution together with a band-diagonal solver (cf. Sect. 3.2.3 in Ref. 1). Since `P3D` is released under GPLv3, we could not use the same intrinsic band-diagonal solver routines as IDL, viz. `LNBCG` and `SPRSIN`, which come from Numerical Recipes. Instead, the C routine solver was implemented using the description of the biconjugate gradient stabilized method that is available on Wikipedia[‡].

3. ADDED FUNCTIONALITY – DATA REDUCTION

To further improve the quality of reduced data we added several new features to the existing set of tools. These features need to be activated either with input keywords or with parameters in the user-parameter file. The new features are discussed in the five following subsections: 3.1, cosmic-ray cleaning in single images; 3.2, recentering offset optimal-extraction cross-dispersion profiles of calibration exposures on science exposures; 3.3, realignment of offset dispersion-mask images of calibration exposures on science exposures; 3.4, modeling and subtraction of scattered light before spectrum extraction; and 3.5, using both twilight flat-field images and lamp flat-field images to normalize extracted spectra.

3.1 Detecting and correcting for cosmic rays in single images

The most straightforward method to remove cosmic rays is to combine several images using some filter. Due to instrument flexure and varying observing conditions during longer exposures such a combination may not be possible. In cases where it – until now – was necessary to remove cosmic rays, an external tool had to be used, such as `L.A. Cosmic` that uses an edge-detection algorithm,⁵ or `DCR` that uses a statistical method.⁶ Only thereafter should any spectra of single images have been extracted with `P3D`. Although, it is often difficult to achieve good results with these methods. Most datasets and parameter combinations result in too few cosmic-ray detections, while many pixels are incorrectly identified as cosmic rays. Until now there have been few options to these two methods.

Husemann, Sandin, Kamann, et al. (in prep.) present a new algorithm – `pyCosmic` – that is tuned to work well with most data of fiber-fed IFSSs; the algorithm is an extended version of `L.A. Cosmic`. Their paper provides a detailed parameter study of the cosmic-ray detection efficiency for all three mentioned algorithms. The outcome reveals that `pyCosmic` in most cases performs extremely well, outperforming the two other algorithms. An arbitrary example of an image section before

[‡]http://en.wikipedia.org/w/index.php?title=Biconjugate_gradient_stabilized_method&oldid=491877806

and after it was cleaned of cosmic rays in `p3d` is shown in Fig. 1. The figure shows that multiple-pixel cosmic rays are removed efficiently. It is in this image more difficult to say something about single pixels (without a detailed statistical study). Both `pyCosmic` and `L.A. Cosmic`[§] are integrated into `p3d`, where they are accessed using the keyword or the user parameter `crClean`, to any of the tools that are used on raw data. All algorithm parameters are available using either keywords or user parameters or both. `p3d` attempts to provide reasonable default values. Nevertheless, it is recommended to check the outcome, and possibly optimize the parameters using the information that is presented in the `pyCosmic` paper. A final note, during optimal extraction `p3d` ignores pixels that are masked as cosmic rays.

3.2 Recentering offset cross-dispersion line profiles on science data before spectrum extraction

Most instruments are to some level affected by flexure, which occurs when the telescope moves across the sky and the instrument along with it. Such flexure results in offsets on the detector on both axes between calibration data and science data. On the CCD the offset can be as high as a few pixels, even over shorter periods of time. This is a critical issue, as accurate optimal spectrum extraction in particular requires extremely accurate line-profile center positions on the cross-dispersion axis; the intensity error in many cases grows fast already with profile offsets that are higher than a tenth of a pixel.¹

An exposure of a continuum light source or the twilight sky are at first used to calculate cross-dispersion line profiles. Between the time of the calibration exposure and the science exposure the spectra are offset. The continuum is, if present, typically much less pronounced in a science exposure, which is why an additional step is required to estimate the offset. `p3d` includes three different approaches to estimate this offset:

Using a median Assume that at least a few spectra contain a continuum. In this case each row of pixels on the dispersion axis can be replaced with a row that was filtered using a wide one-dimensional median. Such a median-filtered image provides a higher accuracy in fitted profile center positions than a single wavelength bin. The filter width is set with the keyword `recenterval` or the user parameter `recentermedwidth`. Any integer value ≥ 3 pixels is accepted, the default width is 20 pixels. An offset is calculated for all (fully working) spectra, but only at a few selected wavelength bins. By default `p3d` uses the center wavelength bin and calculates one median offset from all spectra that is used with all wavelength bins. Additionally, only those spectra are considered where the maximum value is greater than a preset value, by default `recenterlimval=0` [ADU]. Several wavelength bins can be selected using the `recenterdpixpos` parameter to calculate a linear-fit offset as a function of wavelength.

Using an emission line One or more science-object or telluric lines in the spectrum might be bright enough and suitable to estimate a value on the offset. This approach requires a dispersion mask to track the emission lines through all spectra. The default is to select the (approximately) brightest telluric line from the provided high-resolution telluric line-list file; only approximately brightest since a more accurate estimate could be very time consuming. The mode is activated by setting either the keyword `recenterval` to the string “telluric” or the user parameter `recenterusetelluric` to “yes”. Any telluric or object emission line can be selected by setting the keyword `recenterval`, or the user parameter `recentertellines`, to the name of a plain-text file that lists desired lines. Note, that if a science-object emission line is used, which is only available in one or a few spectra, then it is necessary to mask spectra where this line is too faint using the keyword or the user parameter `recenterlimval`. This parameter should be set to a value that indicates a present and bright enough emission line, say `recenterlimval=100`.

Using a pre-determined offset Both the continuum and telluric lines might be too faint if exposure times are very short. In this case the only remaining option is to use either an object emission line, or an offset that was determined for another exposure. A pre-determined offset is set using the keyword `recenterval` or the user parameter `recenteroffset`, where accepted values are $-2.0 \leq \text{offset} \leq 2.0$.

An example that illustrates the need for profile recentering is shown in Fig. 2. The left-hand side panel shows a cross-dispersion cut of science-object raw data at an arbitrary wavelength bin, using PMAS/PPAK IFU data. Without any recentering extracted spectra, which are plotted on top of the raw data, indicate a great loss of accuracy. For some spectra extracted intensities are seemingly off by up to 50 per cent and more. The right-hand side panel shows extracted spectra after recentering; the used offset was about 1 pixel. The improvement in accuracy is drastic. Note that the gained accuracy due to recentering depends on both the instrument as well as observing conditions. Under different circumstances the improvement could be insignificant.

[§]A rewrite of `L.A. Cosmic` was integrated into `p3d` with the permission of P. van Dokkum (Yale) and J. Bloom (UC Berkeley).

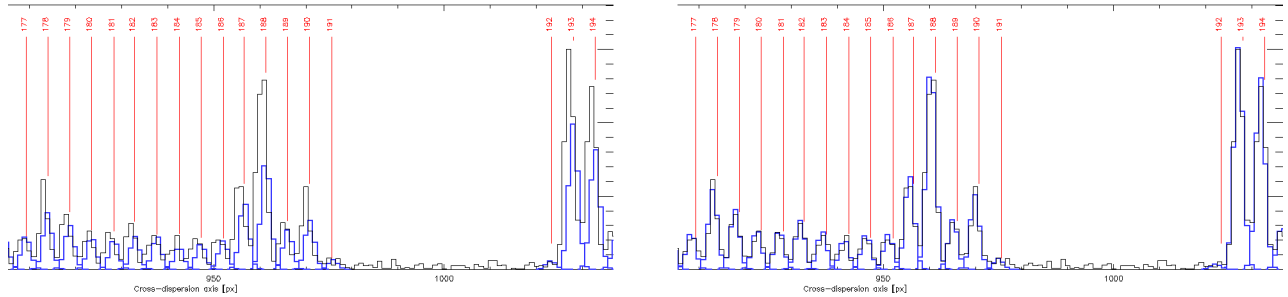


Figure 2. An example of the importance of recentering offset cross-dispersion profiles on science-object data. The black (blue) lines show raw data (extracted spectra) as function of cross-dispersion pixels, and red lines with numbers indicate the spectrum number. Using a section of two separate screenshots the right-hand side (left-hand side) panel shows the result when profiles were (were not) recentered.

3.3 Realignment of the dispersion solution using telluric lines before wavelength calibration

Instrument flexure does not only affect the spectrum-extraction accuracy, which is treated in Sect. 3.2, but it also affects the accuracy that can be attained in the subsequent wavelength calibration. The dispersion solution is calculated using a calibration arc image, and is stored in a so-called dispersion-mask image; this image contains the wavelength as function of pixel for all spectra, in the form of polynomial coefficients. An offset of about one pixel on the dispersion axis seriously affects the accuracy of any kinematic study where the corresponding velocity (offset) is important. The velocity v is related to the wavelength λ and the rest wavelength λ_0 through the Doppler effect:

$$\frac{v}{c} = 1 - \frac{\lambda_0}{\lambda} \quad \text{or} \quad \lambda = \frac{\lambda_0}{1 - v/c},$$

where c is the lightspeed. At $\lambda_0 = 5000 \text{ \AA}$ a one pixel offset results in a 30 km s^{-1} velocity offset for an instrument where the pixel extent is 0.5 \AA . The wavelength to pixel dependence is seldom perfectly linear. Consequently the wavelength offset varies with both the wavelength and the spectrum.

In comparison to science-object emission lines, telluric emission lines are highly suitable when realigning the dispersion mask, since their wavelength is invariable. Provided with a telluric line-list filename, or a wavelength, `p3D` selects all entries that fall within the wavelength range of each spectrum. The line-list filename, or the wavelength, is selected using the keyword or the user parameter `skyalign`. A Gaussian profile is thereafter fitted, for each spectrum, to each entry in the line list, where the initial pixel position is taken from the dispersion mask. For as long as the full width at half maximum of the profile is higher than about two pixels and no blended lines are used, the expected accuracy of the fitted center position is a few hundreds of a pixel. Furthermore, a median wavelength-offset value, which includes all telluric lines and spectra, is calculated and applied to the dispersion mask if the `oneskyoffset` keyword or user parameter is set. The spectra are otherwise treated individually. At first a constant offset is assumed for all pixels on the dispersion axis if one telluric line is specified, otherwise a linear fit is made to the calculated offsets of all telluric lines. In a second step the pixel-offset array is multiplied by a wavelength-extent-per-pixel array. It is possible to set the maximum possible offset, the default value is `maxskyoffset=2.0 [Å]`.

This realignment procedure only works in regions where the dispersion mask was properly calibrated, which is why telluric lines have to be selected in the same region. For example, with VIMOS data using the HR-orange grism it is recommended to avoid the use of the telluric line `[O I] λ5777`, since the arc image that is used to calibrate that wavelength does not contain any lines bluewards of the helium arc line at $\lambda = 5852.488 \text{ \AA}$ (the neon arc line at $\lambda = 5400.56 \text{ \AA}$ is mostly too faint). Conversely, if there are few or very faint telluric lines the attainable accuracy becomes lower. It is advisable to study the outcome carefully, in particular when using two or more telluric lines, to ensure that fitted offsets are reasonable.

3.4 Estimation and subtraction of a scattered-light model before spectrum extraction

With some instruments raw data sometimes show evidence for scattered light, which cannot be corrected using extended cross-dispersion profiles. Such a scattered-light component should vary smoothly across the CCD surface. Regions that are empty of spectra can be used to calculate a model of the scattered-light component, which is subsequently subtracted from the image before spectrum extraction. `p3D` can estimate a model in four steps:

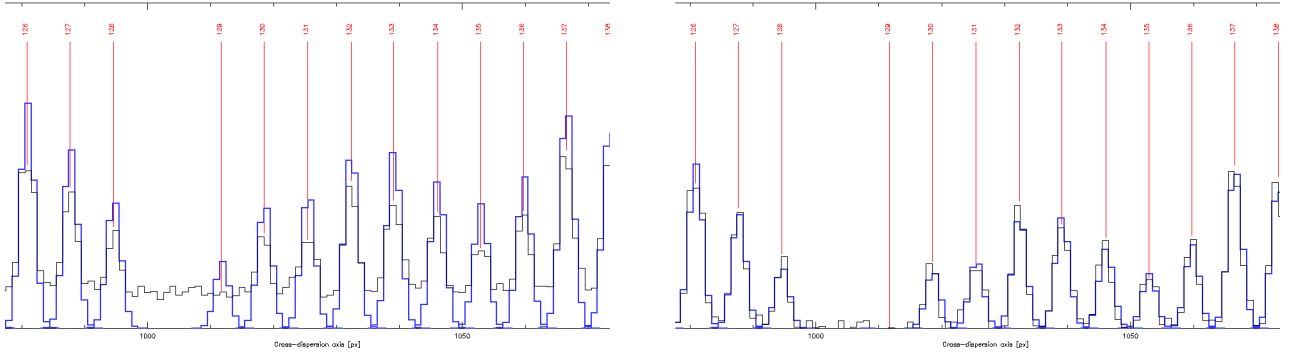


Figure 3. An example of effects of scattered-light subtraction on science-object data. The black (blue) lines show raw data (extracted spectra) as function of cross-dispersion pixels, and red lines with numbers indicate the spectrum number. The ordinate extends across 0–660 [ADU]. Using a section of two separate screenshots the right-hand side (left-hand side) panel shows the result when a scattered-light model were (were not) subtracted from the science-object image.

1. All pixels within a pre-defined distance of each spectrum are masked. The distance is set with the user parameter `sls_maskwidth`, which is divided by the CCD binning value on the cross-dispersion axis bin_\dagger , usually bin_\dagger is 1 or 2; the default is `sls_maskwidth`=1.5 times the profile width. Another requirement is that `sls_maskwidth` $\geq 2\text{bin}_\dagger$.
2. Unmasked regions are smoothed using a median `sls_medfiltern` \times `sls_medfiltern` kernel, the default value is `sls_medfiltern`=20/ bin_\dagger pixels. Masked pixels are ignored in the median calculations. The IDL-routine version of this step is excessively slow, which is why it is performed using a parallelized C routine instead.
3. An interpolated image is calculated for all pixels using unmasked and median-filtered regions. Raw data are fitted with one-dimensional polynomials for one pixel on the dispersion axis at a time; although, the used data array is the dispersion-axis median of a five-pixel wide strip. The polynomial order is defined with the user parameter `sls_polorder`, where the allowed range is $0 \leq \text{sls_polorder} \leq 10$, and the default is `sls_polorder`=7. It is very important to select a polynomial order that makes sense. Only use a high polynomial order if the detector contains sufficiently many empty regions that allow an accurate estimate of the scattered-light contribution.
4. The resulting image of the previous step typically shows plenty of structure on the dispersion axis. In a final step the image is convolved with a Gaussian filter to smooth this structure. The Gaussian-profile width is set with the user parameter `sls_gaussfiltersig`. The default value is 30.0; this step is skipped altogether if it is set to 0.

It is important to check the resulting scattered-light image to check that the model improves the outcome. Set the user parameter `sls_writefile` to `yes` to save this image, check the outcome and adjust the parameters before running the science-object extraction step anew. If it is difficult to calculate a reasonable scattered-light model it might be better to not use it. With some instruments – for example VIMOS – there are no spectrum-free regions on the CCD, which is why it becomes difficult and even impossible to create a scattered-light image. If this should be the case, and there is also a saturated object line in the data the scattered-light estimate is likely too high in parts of the image, resulting in negative intensities. In this case the only option is to use a constant value of the scattered light across the CCD, or to not use this option at all.

An example that illustrates the scattered-light subtraction is shown in Fig. 3. The left-hand side panel shows a cross-dispersion cut of science-object raw data for an arbitrary wavelength bin, using data of the PMAS/LArr IFU and the new $4\text{k} \times 4\text{k}$ CCD. Extracted spectra, which are plotted on top of the raw data, indicate strongly overestimated intensities. The right-hand side panel shows extracted spectra when a fitted scattered-light model was subtracted before spectrum extraction. The improvement in accuracy is significant for all spectra. The subtracted scattered-light model of this case is, moreover, shown in Fig. 4. The image shows plenty of structure on the dispersion axis where the fluctuations between the brightest peaks are less than five per cent, and also a tendency towards more scattered light on the center of the CCD. Note that the gained accuracy depends on both instrument as well as observing conditions. Under different circumstances the amount of scattered light may be lower or higher. The recommended approach is to study different models of a potential scattered-light contribution, before deciding on if it should be modeled and subtracted or not.

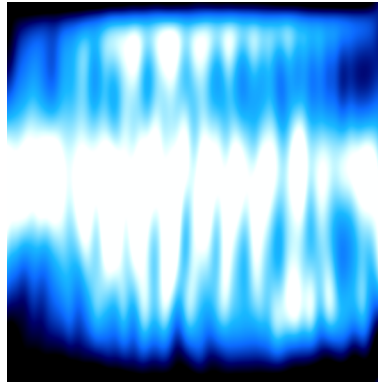


Figure 4. The scattered-light model image that was subtracted from the cross-dispersion cut in the left-hand side panel to produce the cross-dispersion cut in the right-hand side panel in Fig. 3. The dispersion axis is in the horizontal direction. The model reaches down to about 56 ADU in black regions and up to about 72 ADU in white regions.

3.5 Extracted spectra can be normalized using either lamp-flat images or twilight-flat images or both

P3D provides different options when normalizing an extracted science-object image with an extracted flat-field image. Note that the flat-field tool P3D_CFLATF only performs a spectrum extraction, as well as calculates a fiber-to-fiber transmission array. The normalization is only done when object spectra are extracted subsequently with P3D_COBJEX.

At first, extracted spectra are smoothed and replaced with a polynomial fit. This procedure is used to reduce errors in the flat-field data. These tasks are, however, switched off by default with instruments that show time-dependent variations in spectra – so-called fringes – including FLAMES and VIMOS. In a second step a mean spectrum is calculated using fully working spectra only. All spectra are then divided by this mean spectrum, which contains both a fiber-to-fiber correction and a dispersion correction. Moreover, it is possible to use a separate fiber-to-fiber transmission array as input. In this case a fiber-to-fiber transmission array is at first calculated from the current data; this array is used to remove the fiber-to-fiber correction that is achieved in the division by the mean spectrum. In a second step the spectra are multiplied with the separate fiber-to-fiber transmission array and divided by the fiber-to-fiber transmission array of the current data that was calculated in the first step. In a final step the image is divided with its mean value, ignoring masked elements.

Additional care is required if a separate fiber-to-fiber transmission array is used. It is important to exclude regions on the CCD where there is no signal, otherwise these regions might affect the integrated transmission value of individual spectra. Therefore, the lowermost and the uppermost regions of pixels are removed from the input data; this is controlled using the keywords `pcutlow` and `pcuthigh` (to P3D_CFLATF and P3D_COBJEX) or the user parameters `ff_lowerpx` and `ff_upperpx`. The default is to remove five per cent of the total range of pixels at both the lower and the upper end of the CCD. The fiber-to-fiber transmission array is then calculated as follows. For each spectrum the intensity is summed up for all pixels on the dispersion axis, then the summed array of all spectra is divided with its mean value, ignoring any zero-value elements. In this way a fiber-to-fiber transmission array of a twilight flat-field image can be used to renormalize a lamp flat-field image (see above). The outcome is very similar. There is a slight improvement when using the fiber-to-fiber transmission array. For a set of VIMOS data the improvement in flat-fielded data of one detector was found to be up to ten per cent.

4. ADDED FUNCTIONALITY – NEW TOOLS

Often there are several additional steps that should be considered, before reduced science-object data can be used in scientific work. Some of these additional steps that are handled by P3D are described in Sect. 4.1, which discusses how some observational properties are determined in general, and in the following six subsections: 4.2, flux calibration; 4.3, combination of reduced multi-detector data; 4.4, correction for effects of differential atmospheric refraction; 4.5, combination of data using varying exposure times; 4.6, conversion of output data to cube format; 4.7, fitting lines and its visualization. All new tools can be used with the IDL Virtual Machine, thus no IDL license is required.

4.1 Determining observational properties: the airmass, the zenith distance, and the parallactic angle

The airmass, or the zenith distance, is needed both during flux calibration to include effects of extinction and when estimating effects of differential atmospheric refraction. In the latter correction it is also necessary to calculate the parallactic angle. Here we describe how P3D retrieves or calculates these properties. They are calculated mostly using converted versions of FORTRAN routines of the Starlink project.

The parallactic angle is the angle at which the IFU – at zero position angle – is aligned with the direction from the target to the zenith. For some instruments the parallactic angle is available in the file header. The beginning and final parallactic angles are, when available, used to calculate a mean parallactic angle. Otherwise, an available single parallactic angle is used. When the header does not contain any direct information of the parallactic angle it is instead calculated from information on the observatory latitude, the object declination, and the hour angle. The hour angle indicates how much sidereal time has passed since the object was on the local meridian. If the hour angle is unavailable in the header it is calculated using the local sidereal time and the object right ascension. If the parallactic angle is determined separately it can be specified with the keyword `parang` of the tool `P3D_DARC`.

If the header contains both a beginning and a final value of the parallactic angle (higher priority) or the zenith distance (lower priority) then these values are used to first calculate a mean zenith distance, and then beginning value of the airmass, a final value, a mean value, and finally an effective airmass. Otherwise, the beginning and the final header values of the airmass are used to calculate a mean airmass. If there is only one header value of the airmass it is used. If there is only one value of the zenith distance – which can be calculated from the hour angle, the object declination, and the observatory latitude, if it is unavailable in the data header – it is used to calculate the airmass. If the airmass was determined separately it can be specified with the keyword `airmass` of the tools `PD3_FLUXSENS`, `P3D_FLUXCAL`, and `P3D_DARC`.

Some instruments also store the coordinates of a guide star in the object file header, which is used to track an object accurately over extended periods of time. In this case P3D calculates the hour angle, the zenith distance, and the airmass for the guide star separately.

4.2 Flux calibration – P3D_FLUXSENS and P3D_FLUXCAL

All output files that are written by the science-object and flat-field extraction routines in P3D use the analog-to-digital unit (ADU). The conversion to flux units should, if required, be done next. Flux calibration was originally not a part of P3D. Instead the user was encouraged to use the required routines in the Image Reduction and Analysis Facility (IRAF)[¶]. Instructions on how to use IRAF for this purpose are provided at the the P3D documentation wiki. In order to provide a homogenous, extendable, and complete data-reduction tool, P3D now includes tools for flux calibration as well. While preliminary support are included starting with release 2.1.2), more complete support and documentation will be added with the future release 2.2.

The approach in P3D follows IRAF; specifically the routines `STANDARD`, `SENSFUNC`, and `CALIBRATE` of the `ONEDSPEC` package. The prerequisites are an observed wavelength calibrated and sky-subtracted standard-star spectrum, a calibration standard-star spectrum, the atmospheric extinction as function of wavelength, the exposure time t (which is determined using the spectrum file header), and the airmass a (cf. Sect. 4.1). The observed standard-star file must be a fits file that contains one summed spectrum with as much as possible of the standard-star flux; the easiest way to create this file is to use the P3D spectrum viewer. The standard-star calibration spectrum, and the atmospheric extinction file, can be either a fits file or a plain-text file. In either case P3D attempts to setup the proper units of both the wavelength array and the flux array. The units can be specified manually if this attempt is unsuccessful. Internally P3D always uses Angstrom (\AA) for the wavelength and $\text{erg cm}^{-2}\text{s}^{-1}\text{\AA}^{-1}$ for the flux. Data are binned automatically in bandpasses if the calibration standard-star data file contains a column with bandpass widths w_{bandpass} .

The three mentioned files are used with the tool `P3D_FLUXSENS` to create a detector sensitivity function. The method is as follows. A common wavelength range of observed and calibration data is determined. Atmospheric extinction data e_{λ} are interpolated to use the same grid with a rational spline.⁷ The observed spectrum array is interpolated to use the same wavelength array as the calibration data if bandpasses are not used, resulting in f_{λ} . The interpolation is again made using a rational spline. Otherwise, the observed flux is corrected for an extinction gradient within each bandpass. As in IRAF this is done by applying an extinction correction, integrating across the bandpass, and then correcting the integrated intensity

[¶]IRAF is distributed by the National Optical Astronomy Observatories, which are operated by the Association of Universities for Research in Astronomy, Inc., under cooperative agreement with the National Science Foundation.

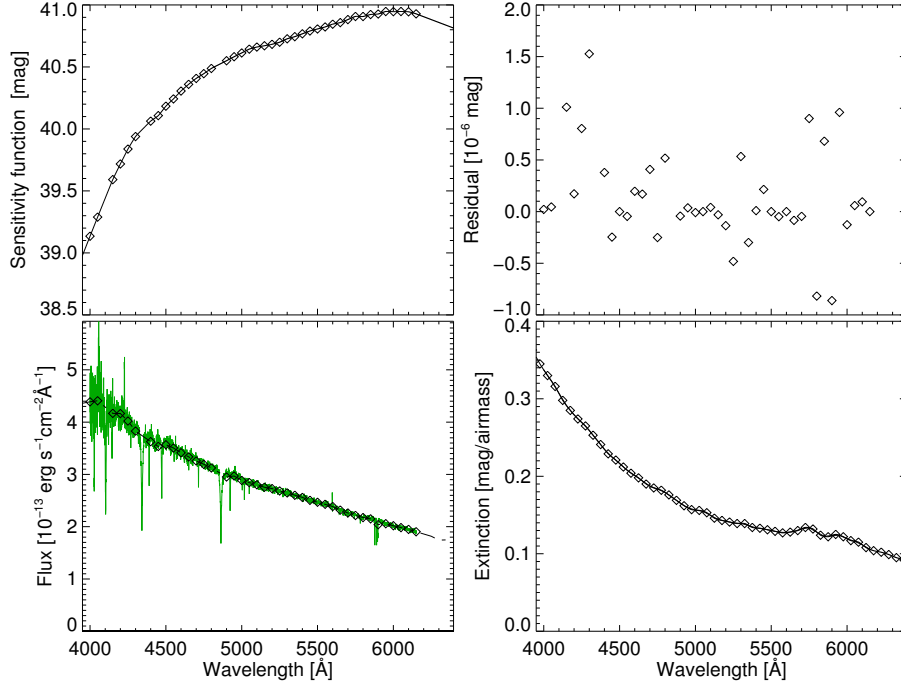


Figure 5. Fitting an observed spectrum of the standard-star Hiltner 600 with a cubic spline. The abscissa shows the wavelength in Angstrom (\AA) for all panels. The top left-hand side (right-hand side) panel shows the sensitivity function (the residual of the fit). The lower left-hand side (right-hand side) panel shows the calibration standard-star spectrum as a green line with the fit overplotted (the extinction). Each symbol shows the center of a bandpass, each 50\AA wide (not shown).

for the extinction at the center of the bandpass. Bandpass entries cannot be edited in the preliminary version, while the final version will allow an interactive removal of unwanted entries. The observed intensities are integrated within a bandpass by co-adding the flux in full pixels and using partial pixels at bandpass edges, resulting in $f_{\text{corr},\lambda}$. A calibration factor c_λ that is expressed in magnitudes is calculated as follows

$$c_\lambda = 2.5 \log \left(\frac{f_{\text{corr},\lambda}}{t f_{\text{cal},\lambda} w_{\text{bandpass},\lambda}} \right) + ae_\lambda \quad \text{and without bandpasses} \quad c_\lambda = 2.5 \log \left(\frac{f_\lambda}{t f_{\text{cal},\lambda}} \right) + ae_\lambda.$$

Finally, a sensitivity function is created by fitting a polynomial or a cubic spline to the calibration factor. A residual is calculated for each bandpass as the difference between the calibration standard-star calibration factor and the fitted standard-star sensitivity function. The polynomial order or the type of function is set using the keyword or the user parameter `inpfuction`. Outside the common wavelength range the calibration factor is extrapolated using a linear function involving the two outermost gridpoints. The sensitivity function is then saved in a fits file. An example of the postscript output of `P3D_FLUXSENS` is shown in Fig. 5. Here an observed spectrum of the standard-star Hiltner 600 has been fitted with a cubic spline to a calibration spectrum for the same star (this file was taken from IRAF). The bandpasses centered on 4100 , 4350 , 4850 , and 6200\AA , were removed by hand in the plain-text calibration standard-star file to improve the quality of the fit. Note that to calibrate spectra that are observed with, e.g., VIMOS or VIRUS-P it is necessary to scale the spectrum to account for light lost between fibers, such scaling is not yet handled automatically by `P3D`.

In a second step science-object data are flux calibrated applying the sensitivity function with the tool `P3D_FLUXCAL`. A correction factor q_λ is calculated for both the atmospheric extinction and the sensitivity function s_λ as

$$q_\lambda = \frac{10^{0.4ae_\lambda}}{tp10^{0.4s_\lambda}},$$

where p is the pixel pitch, i.e. the wavelength extent. Finally, science-object spectra, as well as corresponding error spectra, are multiplied with q_λ , and the resulting spectra are saved in a new fits file.

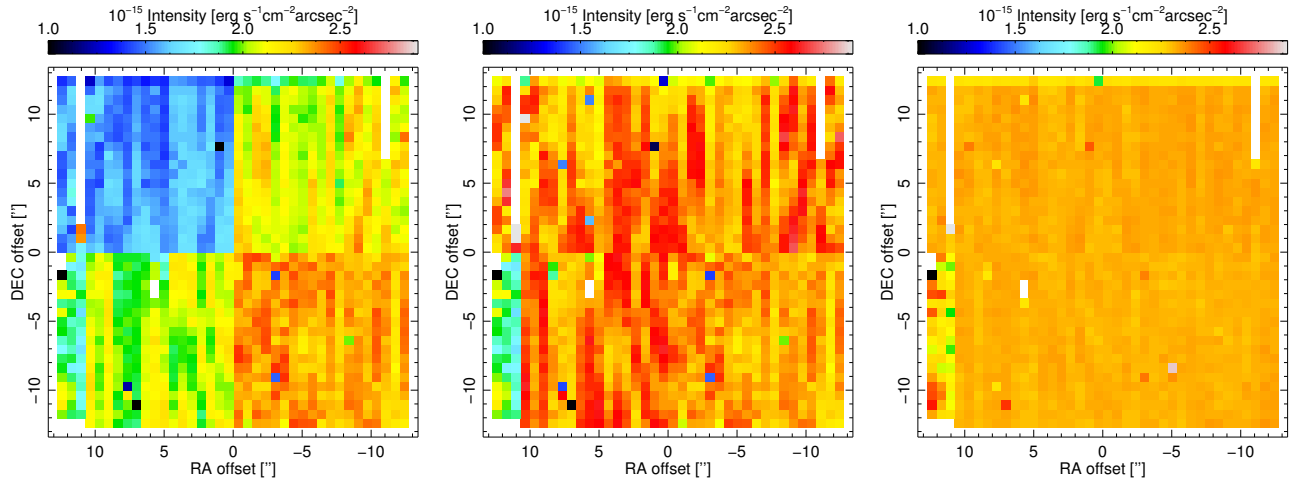


Figure 6. An example showing the effect of renormalization when combining extracted VIMOS data. All panels show the spatial distribution of the integrated intensity of $[O\text{I}]\lambda 5577$. The left-hand side (middle; right-hand side) panel did not use renormalization (used a variant of renormalization; used renormalization). In each panel the top left part is quadrant 1, quadrants 2–4 follow counterclockwise.

4.3 Combination of reduced separate-detector VIMOS data – `p3d_cvimos_combine`

The VIMOS instrument is so far unique in that spectra are grouped into four separate detectors, which are also called quadrants. In the observing modes that are supported by `p3d` – i.e. HR blue, HR orange, HR red, and MR – each detector contains 400 spectra, i.e. 1600 spectra in total. Data are reduced and flux calibrated for each detector individually. Extracted files can be combined with `p3d_cvimos_combine`. At first the four input files are checked that they belong to the same observation block, have the same exposure time (within one second), have the correct number of spectra, have the same wavelength array, and that they are either all flux calibrated or not flux calibrated; this is determined by checking if the maximum value in the extracted image is less than one or greater than one. Furthermore, it is checked that the files belong to different detectors. The same check is made for all error files, if they are available.

If the input files are not flux calibrated data in the respective detector are normalized to use the gain value of the second quadrant. There are more options if data are flux calibrated. In this case all fully working spectra are by default rescaled using fits of the intensity of a telluric line. The telluric line can be selected manually, with the keyword or the user parameter `telluricline`, or automatically. In the latter case the same keyword or user parameter can be used to specify a file that lists telluric lines, otherwise the `p3d` default high-resolution line-list file is used. Thereafter, the brightest line is located out of all line-list entries that fall within 70 per cent of the pixel range on the dispersion axis. It is important to emphasize that the telluric line must be available in all spectra, i.e. it must not have been (completely) removed during the cosmic-ray cleaning procedure. The line should also be bright enough to permit an accurate fit, and there must not be any object emission in the line. Blended lines must also not be used. A Gaussian profile is then fit for each spectrum; spectra of non-working and unused fibers are ignored. A renormalization correction-factor array is calculated for each spectrum by normalizing the fitted intensities against a maximum intensity. The maximum intensity can be set manually, using the keyword or the user parameter `maxintensity`. Otherwise, a median intensity is calculated for each quadrant individually, and the maximum intensity is taken as the maximum value of the four median intensities. An additional possibility is to normalize the intensities per quadrant, by setting the keyword or the user parameter `onlynormquadrant` to `yes`.

Finally, an output spectrum image is created that contains all 1600 spectra. Each spectrum is multiplied by the corresponding correction factor before it is added to the output image. The output image should be used with a corresponding fiber-position table, i.e. `vimos_positions_rer.dat` or `vimos_positions_coc.dat` (if the keyword or the user parameter `keeparrangement` is set).

Figure 6 shows an example that illustrates the effects of renormalization using the telluric line $[O\text{I}]\lambda 5577$. The extracted data of each quadrant were flux calibrated before they were combined. Without renormalization the minimum intensity, in the first quadrant, is about 40 per cent lower than the maximum intensity in quadrant 3. Using the option `onlynormquadrant` the spectra in each quadrant are normalized with the maximum value of the four median fluxes that

are measured in each quadrant separately. In this case the intensity fluctuation is about 20 per cent. When all (fully working) spectra are renormalized individually the intensity fluctuation is less than three per cent.

4.4 Correcting extracted spectrum images for effects of differential atmospheric refraction – p3D_DARC

All observations that are made from the Earth are to some level affected by differential atmospheric refraction (DAR). The consequence is that spatial images at different wavelengths are offset on the detector surface relative to each other. The effect disappears at zenith and increases with the zenith distance, and therefore the airmass. The spatial offset is always in the direction of the parallactic angle, and the offset amplitude can be calculated theoretically from an expression for the refractive index. Assuming a fixed IFU orientation the offset direction varies depending on the time of the observations. IFUs are ideal when correcting for effects of DAR due to their two-dimensional shape. For as long as the airmass is reasonably small, and the exposure time and the wavelength range are reasonably short, the spatial images of each wavelength can be shifted to achieve the same center point. As a consequence there will be rows and columns of spatial elements without any information around the IFU. The width and the height of these rows and columns vary with wavelength.

Two properties are required to shift the spatial image at one wavelength: the parallactic angle that is the offset direction, and the offset amplitude. The shift itself is then performed using a two-dimensional interpolation; the tool p3D_DARC uses bilinear interpolation. The interpolation is straightforward with IFUs that use square-shaped spatial elements (VIMOS, FLAMES/ARGUS, PMAS/LArr, MPFS, and SPIRAL). IFUs that instead use hexagonal- or circular-shaped spatial elements are not yet supported in p3D. In these cases it seems more appropriate to first map the – preferably dithered – intensities on a grid with square-shaped pixels, which is then corrected.

The projected parallactic angle P_{proj} is calculated (following the approach of Walsh & Roy^{8||} as

$$P_{\text{proj}} = s(P - \theta) + P_{\text{offset}},$$

where s is a sign, P the parallactic angle, θ is the IFU position angle, and P_{offset} an optional offset. Not all instruments allow a non-zero IFU position angle. The sign s is negative for FLAMES, GMOS-S, and GMOS-N, and is otherwise positive. P_{offset} is currently set to zero for all supported instruments.

In the theoretical approach the offset amplitude ΔR at wavelength λ is calculated from the refractive index n_λ relative to a reference (pivot) wavelength λ_0 as

$$\Delta R_\lambda = R_{\lambda_0} - R_\lambda \approx (n_{\lambda_0} - n_\lambda) \tan z \text{ [radians]} = 3600 \frac{180}{\pi} (n_{\lambda_0} - n_\lambda) \tan z \text{ [arcsec]},$$

where z is the zenith distance. p3D uses a refractive index that is calculated according to Ciddor⁹ and Edlén;^{10–12} the algorithms are available at the web page of the National Institute of Standards and Technology^{**}. These two expressions for the refractive index deviate slightly from that used by Filippenko,¹³ who uses an older expression. A third and different expression used by Walsh & Roy⁸ is taken from the Starlink-project routine REFRO. This “height-integrated” refractive index is based on the optical/infrared refraction subroutine HMNAO with numerous modifications (cf. the online documentation of REFRO at the Starlink web page^{††}). Three additional properties are required to calculate the refractive index: the air pressure, the air temperature, and the relative humidity. Several instruments include these observing conditions in the header, while for other instruments it is necessary to use some meteorological database, or a logbook, and enter the values manually. Finally, the x and the y axis offsets that are used in the two-dimensional interpolation, Δx and Δy , are calculated as

$$\begin{aligned} \Delta x &= \Delta R_\lambda \Upsilon_x / \zeta \sin P_{\text{proj}} \text{ [arcsec]}, \quad \text{and} \\ \Delta y &= \Delta R_\lambda \Upsilon_y / \zeta \cos P_{\text{proj}} \text{ [arcsec]}, \end{aligned}$$

where ζ is the spatial-element size [arcsec], and Υ is a instrument-specific unit factor, which default value is 1. VIMOS, GMOS, PMAS, and Spiral use $\Upsilon_x = -1$. Currently there is no accounting for correlated noise between pixels; nevertheless, the calculated error should be more precise than an estimate that is made by hand.

A different approach is used by Arribas et al.,¹⁴ who determine both the offset angle and the amplitude by fitting a continuum source for several wavelengths. p3D can also calculate the offset angle and the amplitude using this approach, with the limitation that the object-image must contain a bright star.

^{||}Parts of the DAR-related routine ARSHFT.F, which is found in DAR.tar.gz, are implemented in p3D with the permission of J. Walsh (ESO). The file DAR.tar.gz can be downloaded here <http://ifs.wikidot.com/local--files/walsh-dar/DAR.tar.gz>.

^{**}<http://emtoolbox.nist.gov/Wavelength/Documentation.asp>

^{††}<http://starlink.jach.hawaii.edu>

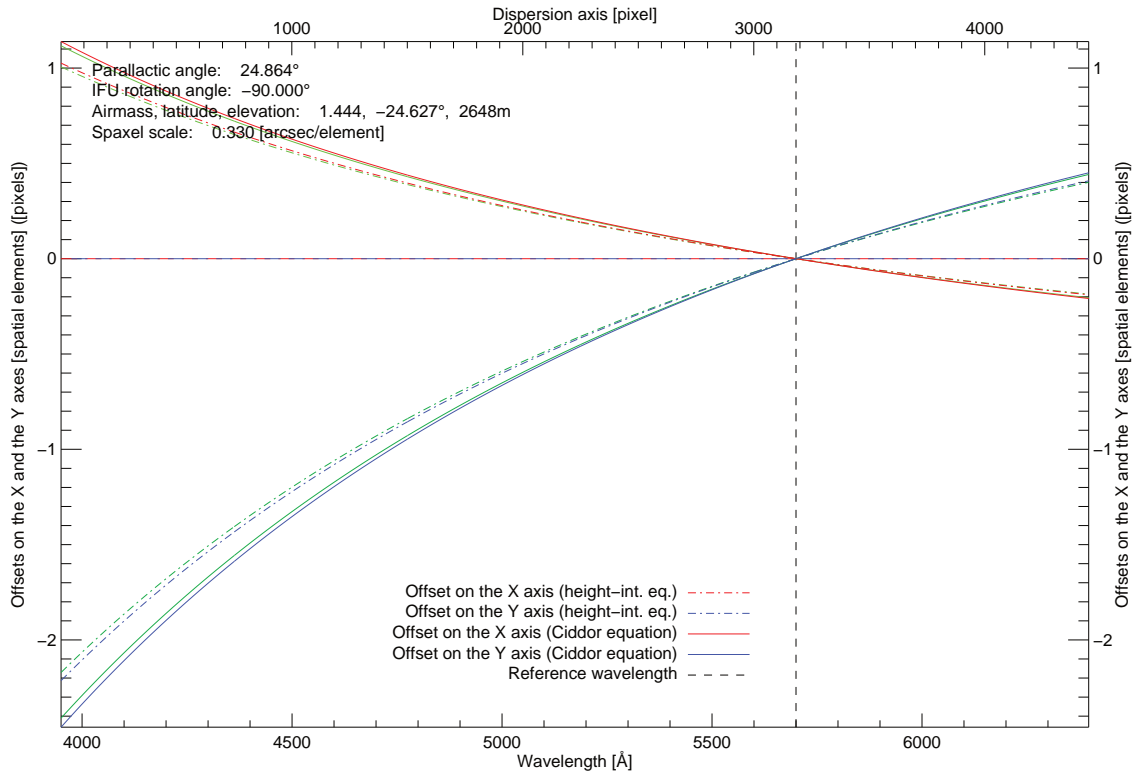


Figure 7. Calculated amplitudes for the correction of DAR with VIMOS data. The offset in pixels is shown as function of wavelength. The green lines, which are nearly parallel to the red and the blue lines, show the corresponding offsets of the guide star.

The theoretical procedure that is outlined above was successfully used to correct observations of planetary-nebula halos in Sandin et al.¹⁵ An example of output of the DAR-correction tool `P3D_DARC` is shown in Fig. 7. Offset arrays were in this case calculated for VIMOS data at airmass 1.44, a reference wavelength of 5700\AA , and the $0'.33$ magnification setup. In this case the air pressure was 740 mbar, the air temperature 10 K, and the relative humidity 13%. The refractive index of Ciddor and the height-integrated equation differ slightly, the Edlén equation nearly coincides with the Ciddor equation and is not seen. The y-axis offset is about two pixels across a wavelength range of 2000\AA , and about one pixel across 1300\AA . The guide-star offsets are very similar to those of the IFU.

4.5 Combination of extracted data that use different exposure times – `P3D_CEXPOSURE`

There are (at least) two reasons to take multiple exposures of the same region on the sky. One reason is that one desires an increased signal-to-noise ratio. In this case one takes several exposures, possibly using different exposure times, which are then combined. A second reason is that one desires complete measurements of an object that shows a large dynamic range; some parts of the object might be saturated at longer exposure times. In the first case shorter exposures could be combined already before spectra are extracted, but this is not recommended with longer exposures. In this latter case observing conditions are likely significantly different for the separate exposures. Important effects that affect observations include instrument flexure and DAR, which both vary with time. In the latter case it is therefore recommended to combine the exposures after they have been extracted and corrected. Here we describe how exposures can be combined with the tool `P3D_CEXPOSURE`, in either case.

In a first step `P3D` checks that all input files exist and use the same wavelength array, and that they have the same number of spectra. The exposure time must be different in all files if the keyword `saturated` is set, but can differ otherwise. If the corresponding error files are found they are also checked. The spectra are combined with the exposure time as a weight when `saturated` is unset, this is the default.

The second case is used if the keyword `saturated` is set, but in this case `p3d` needs to know which spectra are saturated, before the images are combined. During spectrum extraction `p3d` can create a mask that indicates which input raw-data pixels are saturated; this applies to the three tools `P3D_COBJEX`, `P3D_CFLATF`, and `P3D_CDMASK`. This mask is written when the keyword `satmask` is set, or the user parameter `writesatmask` is set to `yes`. The default saturation level is 45,000 [ADU], which can be modified with the user parameter `satlimit`.

The images are then sorted with decreasing exposure time t , along with the respective saturated-pixels mask image. The image with the longest exposure time is used as reference. For each spectrum in the reference image, all pixels p in the range $p - dp \leq p \leq p + dp$ are masked to be replaced with the corresponding pixel value in the next shorter exposure. The pixels p are the previously masked pixels of the current spectrum in the saturated-pixels mask image. The default value of dp is 30 pixels, which can be changed with the keyword `pixrange`. Before masked spectrum pixels of the shorter exposure are inserted in the reference image they are multiplied with the scaling factor $t_{\text{reference}}/t_{\text{shorter}}$. The procedure is repeated for all shorter exposures.

4.6 Converting resulting row-stacked-spectrum images into cubes – `P3D_RSS2CUBE`

Extracted spectrum images are always saved in the so-called row-stacked-spectrum (RSS) format. Here each row or column in the two-dimensional image, depending on the chosen dispersion axis, is a spectrum. To create a spatial map at any wavelength it is necessary to use a fiber-position table that contains information on where on the sky each spectrum is positioned. Alternatively, `p3d` can also save output data in the E3D format,¹⁶ which includes a fiber-position table in the first fits-file extension. Also, fiber-position tables that are prepared for use with the `PINGSOFT`¹⁷ tool are provided since release 2.1.1. Note, however, that current versions of `PINGSOFT` only accept the horizontal axis as dispersion axis. Therefore, with instruments that use the vertical axis instead it is necessary to transpose the RSS images, including the wavelength-array information keywords, before they are used with `PINGSOFT`.

`p3d` can for some instruments convert the RSS image and its error image into a three-dimensional cube with the tool `P3D_RSS2CUBE`, where the wavelength is in the third dimension. Specifically, this can be done for all instruments that use square-shaped spatial elements – i.e. `VIMOS`, `FLAMES/Argus`, `PMAS/LArr`, `MPFS`, and `SPIRAL`. The cube is, if possible, rotated to have North upwards and East leftwards. Some instruments allow a non-zero IFU position angle. The cube is rotated only when the rounded position angle is a multiple of 90 degrees. Furthermore, by default all pixels on the dispersion axis are included in the cube. It is possible to delimit the pixel (wavelength) range with the keywords `pixstart` and `pixend` (`wavestart` and `waveend` [Å]); a wavelength delimiter is ignored if a pixel delimiter is specified. The resulting cube can be loaded directly into `SAOImage DS9`.

It is also possible to save up to ten spatial-map images in a data cube from the spectrum viewer. At first, select desired wavelengths and save the spatial map on the small-image middle row with a mouse click. Thereafter, select the menu entry “Save spatial maps” in the file menu.

4.7 Fitting lines and creating plots for publication – the `P3D_IFSFIT` package

After spectra have been extracted and corrected they can be analyzed. For as long as velocities are moderate it is possible to fit emission lines with profiles to extract integrated intensities. At high velocities, which are found in e.g. supernovæ, this becomes tricky since closely spaced lines likely blend into each other. The integration of line intensities is cumbersome with IFS data, since the same fitting procedure has to be repeated for up to several thousand spectra. `IFSFIT` is a new tool for `p3d` that does this work for extracted data (Sandin, in prep.). Features of `IFSFIT` include:

Simple configuration file Everything related to the configuration of any number of lines is specified in a plain-text file. The format allows `IFSFIT` to be automatically configured and launched from another tool.

Several wavelength regions Each line is assigned a wavelength-region group. Any number of such groups and extents can be specified in the same configuration file.

Emission lines and absorption lines Any combination of emission lines and absorption lines is accepted, including line blends. The only required input is the rest wavelength. The absorption-line type must be specified, if such lines are used. Any wavelength can only be used by one line, unless one is an emission line and the other an absorption line.

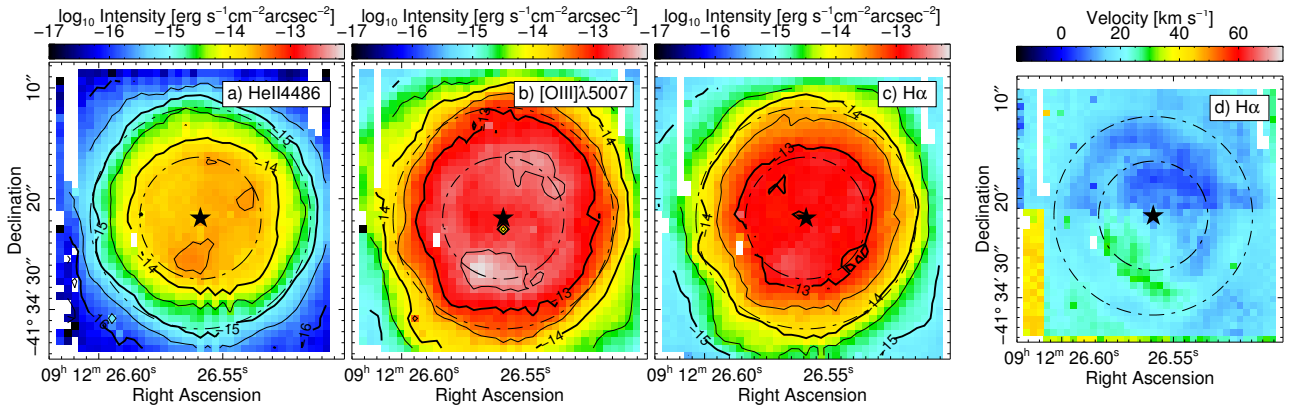


Figure 8. Example of figures that are produced by `IFSFIT`. Panel **d**) shows a velocity field and panels **a**)-**c**) intensity fields; these three panels all use the same colortable where the intensity uses a logarithmic scale. The field is centered on the central star (marked with a star symbol) of the planetary nebula NGC 2792. The axes use a sexagesimal coordinate representation, and the dash-dotted circles indicate the previously measured locations of the so-called rim and shell.

Fixed relative wavelengths Line wavelengths are by default fixed relative to each other. The relative separations between lines can be allowed to vary, if separations vary due to, for example, kinematic differences. In such cases the relative separations can be allowed to vary. Fitted wavelengths are allowed to deviate by a preset value from the respective rest wavelength, by default this value is 1.0\AA . A redshift is specified with the keyword with the same name.

Use different profile functions Currently four profile functions are available: the 3-parameter Gaussian and Lorentzian profiles, and the 4-parameter Moffat and parameterized Voigt profiles.

Continuum The continuum is fitted with a linear polynomial of order 0–3.

Sky emission lines Sky-emission lines could, if present, be indicated as such. These lines are not redshifted with the other lines. Unless they are too many, properly setup sky-emission lines could help to fit the continuum accurately.

Use individual or binned fits All spectra, including those of low-transmission fibers, but excluding non-working or unused spectra, are by default handled individually. It is also possible to provide a binning map, which allows `IFSFIT` to group spectra into bins, before any lines are fitted.

Always check the quality of the fit The quality of each fit can be inspected in quality-check postscript files. Additionally, a supplied graphical-user-interface tool can be used to inspect each fit more closely, and also mark unsuccessful fits.

For each individual line entry all fitted parameters are written to a binary-table fits file. Other tools are provided to visualize integrated properties. Such properties could be intensities, velocities, as well as other derived properties. The tool also plots contours, and allows full customization of axes, labels, colortables, and colorbars. Mosaics are easily created by specifying a spatial offset for each image, and any number of plots can be stacked both horizontally and vertically. `IFSFIT` will be included in `P3D` beginning with the future release 2.3.

Figures 6 & 8 show examples of `P3D_IFSFIT` output for VIMOS data. The white frame around each panel appears as those spectra are vignetted. Thicker borders in Fig. 8 occur during the DAR correction. The velocity structure in Fig. 8d shows very small differences that are smaller than the velocity extent of one pixel. The jagged structure that is visible in the middle lower part of Fig. 8a, in particular, is caused by the third quadrant; where spectra in the blue part of the CCD are out of focus and even inseparable in the raw data.

5. CONCLUSIONS

In this paper we have presented numerous improvements to the open-source data-reduction tool `P3D`. These improvements have been made to drastically simplify the reduction process of data from fiber-fed integral-field units. New functionality

has been added to existing reduction tools. Notably, p3d can now clean single images of cosmic rays, recenter data on both axes that were offset due to instrument flexure, estimate and subtract a scattered-light model, and use both twilight and lamp flat-field images. New tools have been added to do flux calibration, combine extracted images of the multi-detector instrument VIMOS, correct for differential atmospheric refraction (DAR), combine extracted spectrum images, convert output images to cubes, and fit and visualize any combinations of emission and absorption lines.

However, there is still more work to do that can further improve the quality of reduced data. Additional instruments can be supported, and more tasks can be added. For example, the error calculation of DAR-corrected images could be made more accurate through consideration of correlated noise. We would use a similar approach as Weilbacher et al.,¹⁸ who use a so-called pixel table, to never interpolate data more than once. As a final remark, we consider adopting the sky-subtraction procedure that is currently being developed for the MUSE instrument.¹⁹

ACKNOWLEDGMENTS

C.S. was supported by the grant PTDESY-05A12BA1.

REFERENCES

- [1] Sandin, C., Becker, T., Roth, M. M., Gerssen, J., Monreal-Ibero, A., Böhm, P., and Weilbacher, P., “p3d: a general data-reduction tool for fiber-fed integral-field spectrographs,” *A&A* **515**, A35 (June 2010).
- [2] Becker, T., *3D Spektroskopie hintergrundkontaminierter Einzelobjekte in Galaxien der lokalen Gruppe*, PhD thesis, Univ. Potsdam (2001).
- [3] Fruchter, A. S. and Hook, R. N., “Drizzle: A Method for the Linear Reconstruction of Undersampled Images,” *PASP* **114**, 144–152 (Feb. 2002).
- [4] Sandin, C., Weilbacher, P., Streicher, O., Walcher, C. J., and Roth, M. M., “p3d – A Data Reduction Tool for the Integral-field Modes of VIMOS and FLAMES,” *The Messenger* **144**, 13–16 (June 2011).
- [5] van Dokkum, P. G., “Cosmic-Ray Rejection by Laplacian Edge Detection,” *PASP* **113**, 1420–1427 (Nov. 2001).
- [6] Pych, W., “A Fast Algorithm for Cosmic-Ray Removal from Single Images,” *PASP* **116**, 148–153 (Feb. 2004).
- [7] Späth, H. and Meier, J., [*Eindimensionale Spline – Interpolations Algorithmen*], Oldenbourg Verlag (1990).
- [8] Walsh, J. R. and Roy, J. R., “Area Spectroscopy and Correction for Differential Atmospheric Refraction,” *Proc. ESO* **34**, 95–99 (1990).
- [9] Ciddor, P. E., “Refractive index of air: new equations for the visible and near infrared,” *Applied Optics* **35**, 1566–1573 (Mar. 1996).
- [10] Edlén, B., “The refractive index of air,” *Metrologia* **2**, 71–80 (1966).
- [11] Birch, K. P. and Downs, M., “An updated Edlén equation for the refractive index of air,” *Metrologia* **30**, 155–162 (1993).
- [12] Birch, K. P. and Downs, M., “Correction to the updated Edlén equation for the refractive index of air,” *Metrologia* **31**, 315–316 (1993).
- [13] Filippenko, A. V., “The importance of atmospheric differential refraction in spectrophotometry,” *PASP* **94**, 715–721 (Aug. 1982).
- [14] Arribas, S., Mediavilla, E., García-Lorenzo, B., del Burgo, C., and Fuensalida, J. J., “Differential atmospheric refraction in integral-field spectroscopy: Effects and correction. Atmospheric refraction in IFS,” *A&AS* **136**, 189–192 (Apr. 1999).
- [15] Sandin, C., Schönberner, D., Roth, M. M., Steffen, M., Böhm, P., and Monreal-Ibero, A., “Spatially resolved spectroscopy of planetary nebulae and their halos. I. Five galactic disk objects,” *A&A* **486**, 545–567 (Aug. 2008).
- [16] Kissler-Patig, M., Copin, Y., Ferruit, P., Pécontal-Rousset, A., and Roth, M. M., “The Euro3D data format: A common FITS data format for integral field spectrographs,” *Astronomische Nachrichten* **325**, 159–162 (Mar. 2004).
- [17] Rosales-Ortega, F. F., “PINGSOFT: An IDL visualisation and manipulation tool for integral field spectroscopic data,” *New Astronomy* **16**, 220–228 (Apr. 2011).
- [18] Weilbacher, P., Streicher, O., Urrutia, T., Jarno, A., Pécontal-Rousset, A., Bacon, R., and Böhm, P. “Design and capabilities of the MUSE data reduction software and pipeline,” *Proc. SPIE* **8451**, in press (2012).
- [19] Streicher, O., Weilbacher, P. M., Bacon, R., and Jarno, A., “Sky Subtraction for the MUSE Data Reduction Pipeline,” in [*ADASS XX*], Evans, I. N., Accomazzi, A., Mink, D. J., and Rots, A. H., eds., *ASP Conf. Ser.* **442**, 257–260 (July 2011).